Chapter 3

Polysiloxane Side-Chain Azobenzene-Containing Liquid Single Crystal Elastomers for Photo-Active Artificial Muscle-Like Actuators

Jaume Garcia-Amorós and Dolores Velasco

Additional information is available at the end of the chapter

http://dx.doi.org/10.5772/50436

1. Introduction

Liquid crystals (LCs) are unique materials with amazing properties and uses. Since their discovery in 1889 by F. Reinitzer[1], they have experienced an explosive growth because of their successful application in a wide variety of areas such as information displays[2], cosmetics and health care[3], thermography[4-5], artificial muscle-like actuators[6-7] and enantioselective synthesis[8], among others. Thus, liquid crystals play an important role in modern technology and they are present in the most common devices used in our daily live. Research into this field is growing day by day and new promising applications for such materials are discovered and developed continuously.

The liquid-crystalline state or mesophase is a different state of condensed matter, which is intermediate between solids and liquids (**Figure 1**).[9] Liquid-crystalline materials combine both the molecular order typical of the solid phases and the fluidity characteristic of the isotropic liquid state. Compared with conventional liquids, liquid crystals exhibit long-range orientational order and, in some cases, some partial positional order. Although the degree of order present in a mesophase is lower in comparison to that in conventional solids, it is high enough to induce a great anisotropy in the properties of the system. Hence, liquid crystals are fluids with anisotropic properties because of the mesogens tendency to point to a common direction called director, ***n***.

Liquid-crystalline elastomers (LCEs) consist on high-molecular mass liquid crystals where the mesogenic moieties can be connected either head-to-tail, forming the polymer main chain (main-chain LCEs), or attached as side-chain groups to the main polymer backbone (side-chain LCEs), generally *via* flexible spacers, which allow the polymer main chain to accommodate the anisotropic arrangement of the mesogenic side groups (**Figure 2**).[10-11]

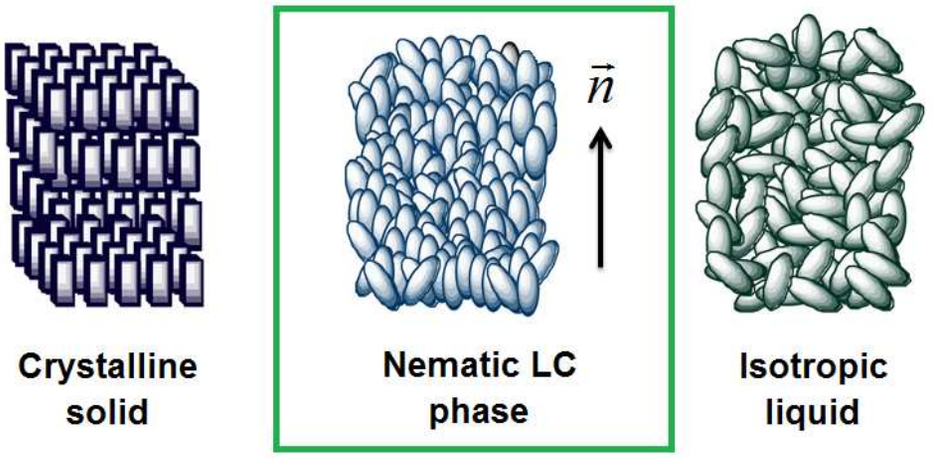

Figure 1. Schematic representation of the molecular distribution in the solid, nematic liquid-crystalline and liquid state, respectively.

Among all liquid-crystalline phases, the nematic one, where the mesogens are approximately oriented parallel to their longest axis, is the less ordered and, therefore, the less viscous. As a consequence, the mesogens alignment can be more easily manipulated than in the more ordered ones. Hence, nematic liquid-crystalline materials are the most commonly used for technical applications. Specifically, this chapter focuses on the photo-actuating properties of nematic liquid-crystalline elastomeric materials.

The properties of liquid-crystalline materials can be easily modulated by applying external perturbations such as light, temperature, electro-magnetic fields, changes of solvent or pH, and so on, which induce changes in the molecular and supermolecular organization of such systems. This feature is the basis of all their further applications.[12-13]

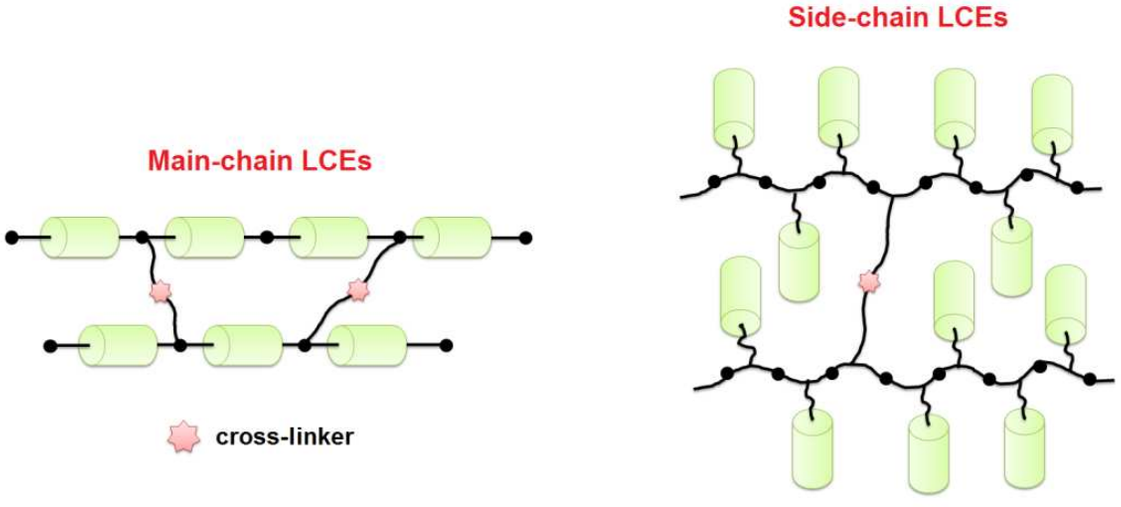

Figure 2. Main-chain (left) and side-chain (right) liquid-crystalline elastomeric materials.

Among all the possible external inputs, light enables a rapid and punctual wireless control of the properties of the material and, moreover, it is a clean, cheap and environmentally-friendly energy source. Several chromophores are known in photochemistry: spiropyranes,

diarylethenes, fulgides, stilbenes, viologens, *etc*. However, azobenzenes are doubtlessly the most used ones for designing optically-controlled materials because of their totally clean and reversible isomerisation process between their two isomers of different stability: *trans* and *cis*. The most interesting feature of azobenzenes is that both isomers can be switched back and forward with light of particular wavelengths: UV light ($h\nu_1$), for the *trans*-to-*cis* conversion, and visible light ($h\nu_2$), for the *cis*-to-*trans* isomerisation. Moreover, *cis* isomer is less stable than the *trans* one because it has a bent shape which increases the steric hindrance and somehow breaks the conjugation of the *trans* linear form. Thus, the metastable *cis* isomer will also relax back spontaneously to the thermodynamically stable *trans* form in the dark isothermally (Δ, **Figure 3**).[14]

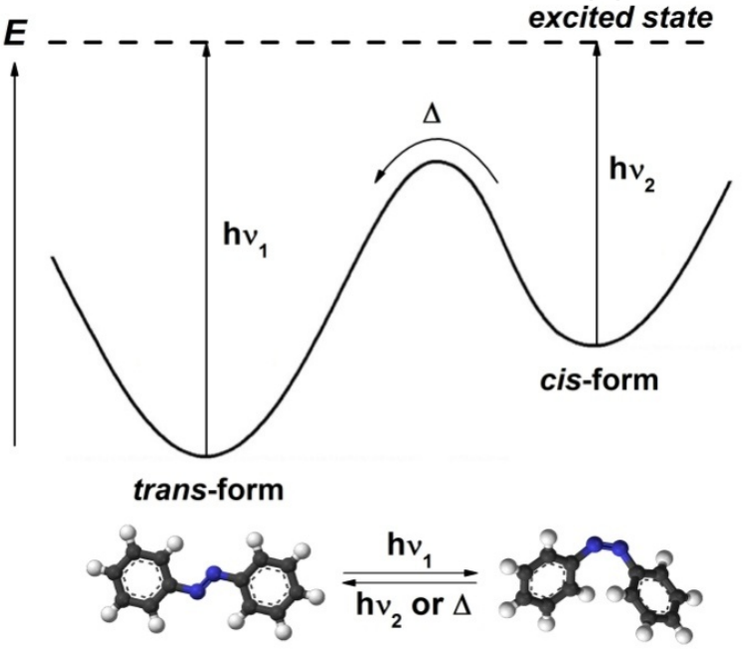

Figure 3. Photochromism of azobenzene and energetic profile for its *trans*-to-*cis* and *cis*-to-*trans* isomerisation processes.

The rod-like structure of *trans*-azobenzene allows its easy introduction in both low- and high-molecular mass nematic liquid crystals without causing the destruction of the host mesophase. When the system is irradiated with light of the appropriate wavelength ($h\nu_1$), the bent *cis* form is generated. As a consequence, the orientation of all the mesogenic molecules of the sample will also change (domino effect). In this way, the *cis* azo-moiety acts as an impurity lowering the nematic order. This effect can be nicely observed experimentally when azobenzene-doped liquid-crystalline mixtures are irradiated at a constant temperature, T, within $T_{\text{N-I (trans)}}$ and $T_{\text{N-I (cis)}}$. In this case, the sample changes from the ordered nematic phase to the disordered isotropic one isothermally, that is, a photo-induced nematic-to-isotropic phase transition occurs (**Figure 4 and 5**).[15-17] The initial state is restored on turning off the irradiation due to the thermal back *cis*-to-*trans* isomerisation of the azo-dye in the dark (Δ).[18] This effect can be exploited for obtaining promising light-controlled liquid-crystalline materials such as photo-active artificial muscle-like actuators and light-driven optical switches.

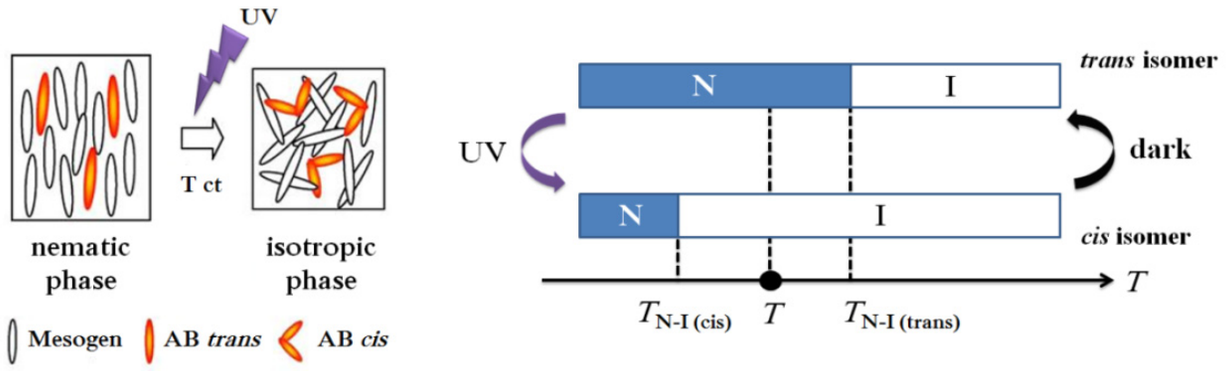

Figure 4. Photo-induced nematic-to-isotropic phase transition in azobenzene-doped nematic liquid crystals.

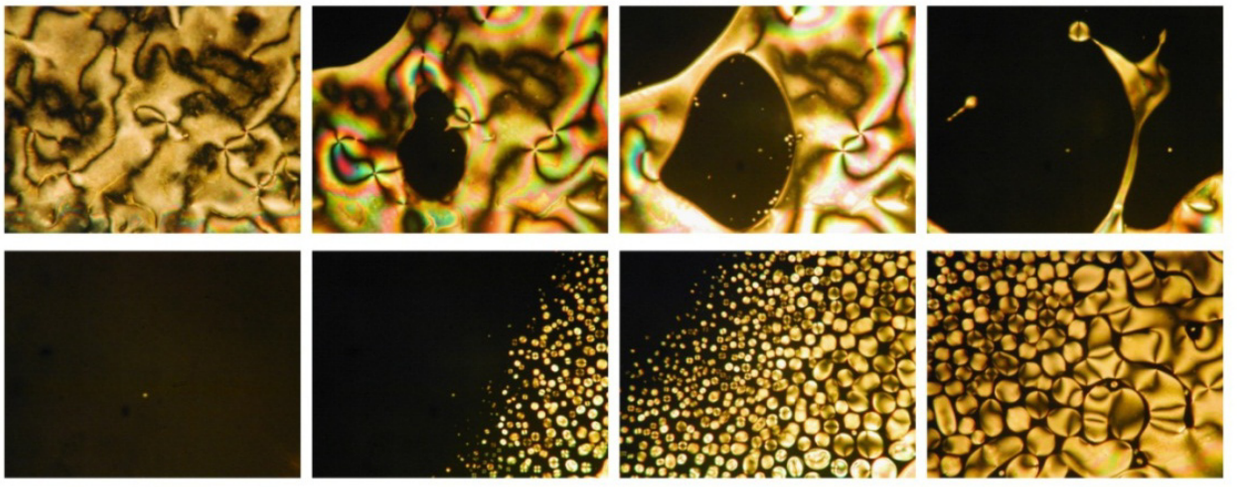

Figure 5. Photo-induced nematic-to-isotropic phase transition in an azobenzene-containing nematic liquid-crystalline mixture. Destruction of the host nematic mesophase by irradiation with UV light at a constant temperature T between $T_{N\text{-}I\ (cis)}$ and $T_{N\text{-}I\ (trans)}$ (up). Regeneration of the nematic mesophase when the thermal *cis*-to-*trans* relaxation of the azobenzene occurs in the dark (down).

2. Liquid-crystalline elastomers for light-induced artificial muscle-like actuation

Photo-active artificial muscle-like actuators convert light into mechanical quantities such as displacement, strain, velocity and stress. Moreover, materials used to produce muscle-like movements should be soft and deform easily upon irradiation. Specifically, polymers are very interesting materials for this purpose due to their many attractive properties and characteristics; they are lightweight, inexpensive, easily manufacturable and implementable, fracture tolerant, pliable and biocompatible.[19] So, light-driven polymer-based actuators are valuable materials to be implemented in a wide range of micro- and macro-scale devices.

Generally, photo-active liquid-crystalline polymers and elastomers are multidomain systems and, therefore, the director changes abruptly from one domain to another. Hence,

both LCPs and LCEs deform themselves when non-polarised light falls on them in an isotropic way, that is, there is no preferential direction for the deformation and, as a consequence, the degree of deformation of the material is generally small.[20]

Highly noteworthy photo-actuating properties have been successfully achieved in polydomain azobenzene-based liquid-crystalline elastomeric materials by Ikeda.[21-26] These materials show a great variety of three-dimensional contraction and expansion movements when they are exposed to polarised light of the appropriate wavelength. Within the last few years, it has been reported that it is possible to control the bending direction of the LCE film depending on the role of the azoderivative within the elastomeric network, that is, if the azo-chromophore acts as a cross-linker or as a simply pendant group.[27] Moreover, the first prototypes of real light-controlled plastic rotating motors have been fabricated with laminated films of photo-sensitive LCEs.[28]

However, if non-polarized light is used instead, it is strictly necessary that the director points to a unique direction in the whole sample, that is, a monodomain sample is required.

Liquid single crystal elastomers (LSCEs) are a subclass of liquid-crystalline polymers, which were synthesized for the first time by Küpfer and Finkelmann in the early nineties[29], although their possible use for both thermally- and photo-controlled artificial muscles was predicted earlier theoretically by P. G. de Gennes.[30] LSCEs consist in weakly cross-linked polymer networks with a macroscopic orientation of the director, ***n***. These materials combine the elasticity typical of conventional rubbers with the anisotropic properties characteristic of liquid-crystalline systems. As a result of this coupling, the macroscopic dimensions of the elastomeric sample can be easily modified by the appropriate modification of the LC order through the application of different external stimuli such as temperature variations or, when an azo-dye is introduced in the system, by irradiating the probe with light of the appropriate wavelength.[31]

Indeed, LSCEs experiment a spontaneous contraction along the director direction when the system is driven from the ordered nematic phase to the disordered isotropic one by heating the sample over the nematic-to-isotropic phase transition temperature, $T_{N\text{-}I}$, due to the mesogens misalignment. If the temperature is lowered below $T_{N\text{-}I}$, the LSCE expands back thereby recovering its original shape. This effect is the so-called thermo-mechanical effect (**Figure 6a and 7**).[32-36]

The introduction of photo-sensitive azoderivatives in LSCEs, not only as side-chain groups but as cross-linkers as well, affords a new way to control the macroscopic dimensions of the sample isothermally just by applying light. So, azobenzene-containing LSCEs are very attractive materials for the fabrication of light-controlled artificial muscle-like actuators.[37-38] During the last decades, both the preparation and properties modulation of light-driven artificial muscle-like actuators based on azobenzene-containing LSCEs are topics of intensive research. Thus, in this chapter we will describe the last investigations that have been performed in our group towards not only to enhance the mechanical efficiency of such materials but also to optimise the response time of the final artificial muscle.

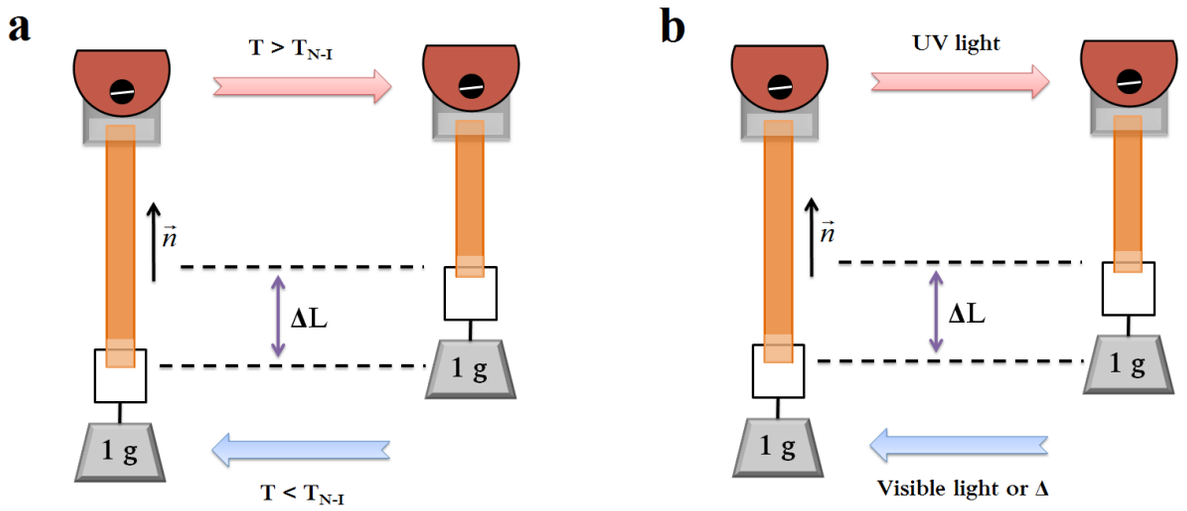

Figure 6. Thermo-mechanical (a) and opto-mechanical (b) effect in nematic LSCEs.

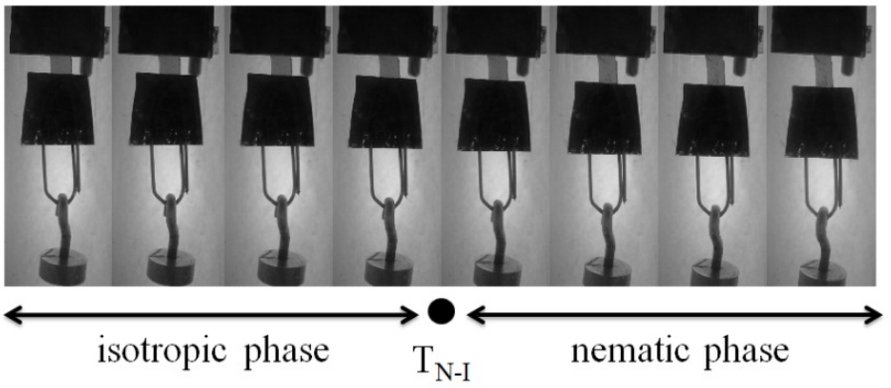

Figure 7. Uniaxial thermal expansion of an LSCE sample on lowering the temperature as a consequence of the isotropic-to-nematic phase transition.

Besides the thermo-mechanical effect commented above, LSCEs that contain isomerisable azobenzenes as light-sensitive molecules also undergo macroscopic contractions in a preferential direction when they are exposed to non-polarised light of the appropriate wavelength (opto-mechanical effect, **Figure 6b**). This happens due to the *trans*-to-*cis* isomerisation of the azo-dye, which drops the nematic order parameter of the elastomeric sample.[38] On turning off the light, the system recovers its initial dimensions due to the thermal back isomerisation of the azo-chromophore. Photo-mechanical effect in nematic LSCEs was first observed by Finkelmann *et al.*[39] in 2001 and it has been deeply investigated during the last decade from both the theoretical and the experimental point of view. A mathematical description of the opto-mechanical effect will be given in Section 4 of this chapter.

3. Preparation and characterization of polysiloxane-based liquid single crystal elastomers

As it has been commented above, both low- and high-molecular mass liquid crystals present different domains and, therefore, there are some places in the sample where the director

changes abruptly. However, for many applications like artificial muscle-like actuation, it is strictly necessary that the system should be macroscopically oriented, *i.e.* a monodomain sample used.

Several techniques are used for this purpose with low-molecular mass LCs like rubbing, surface treatments with polymers or the application of external fields in a determined direction. High-molecular mass LCs, like linear LCPs, can be macroscopically oriented by extruding the polymeric mass in order to create very thin oriented fibres. However, this technique is not useful for LCEs. In such systems, the macroscopic orientation of the sample should be carried out during its preparation.

Many smart and functional liquid-crystalline elastomeric materials have been prepared using different polymer backbones. However, silicone is doubtlessly one of the most commonly used polymer backbone for preparing LSCEs due to its great advantages like good thermal stability, constancy of properties over a wide range of temperature which leads to a large operating temperature range – from −100 to 250 ºC –, hydrophobicity, excellent resistance to oxygen, ozone and sunlight, good flexibility, anti-adhesive properties and low toxicity. An additional noteworthy point is that silicone polymers, of which polyhydrogenomethylsiloxane is an example, have very low glass transition temperatures (*ca*. T_g = −120 °C). This feature allows polysiloxane-based LSCEs to present photo-actuation even at room temperature.

Generally, polysiloxane-based side-chain liquid single crystal elastomers are prepared following the synthetic methodology in three steps, which was first developed by Küpfer and Finkelmann (**Figure 8**).[29]

In the first step, the different monomers, those are, mesogen/s, cross-linker/s and comonomer/s, react through their terminal olefin with the polysiloxane backbone through a Pt-catalysed hydrosilylation reaction which takes place at 70 °C (**Figure 9**). This reaction is carried out at 5000 rpm by means of the spin-casting technique. The aim of this step is to obtain a stable elastomeric system, which can be handled properly, but partially cross-linked for its further macroscopic orientation. For this purpose, the hydrosilylation reaction is stopped before it is completely finished.

In the second step, the orientation of the different directors of the entire sample is performed. This process is induced by the application of a uniaxial force to the sample along its longest axis. After the suitable time, a monodomain LCE is obtained, that is, a liquid single crystal elastomer (LSCE). The progress of the orientation process can be followed qualitatively *in situ* by checking the optical transparency of the probe. When the orientation of the director of the different domains is successful, one gets an LSCE, which is perfectly transparent (**Figure 10a**). Contrarily, if a macroscopically disordered sample is obtained, it will show opacity due to the scattering of the incoming light through the sample (**Figure 10c**).

As it has been aforementioned, macroscopic changes in shape are coupled to changes at the molecular scale. Hence, the deformation of an elastomer can lead to reorientation of the

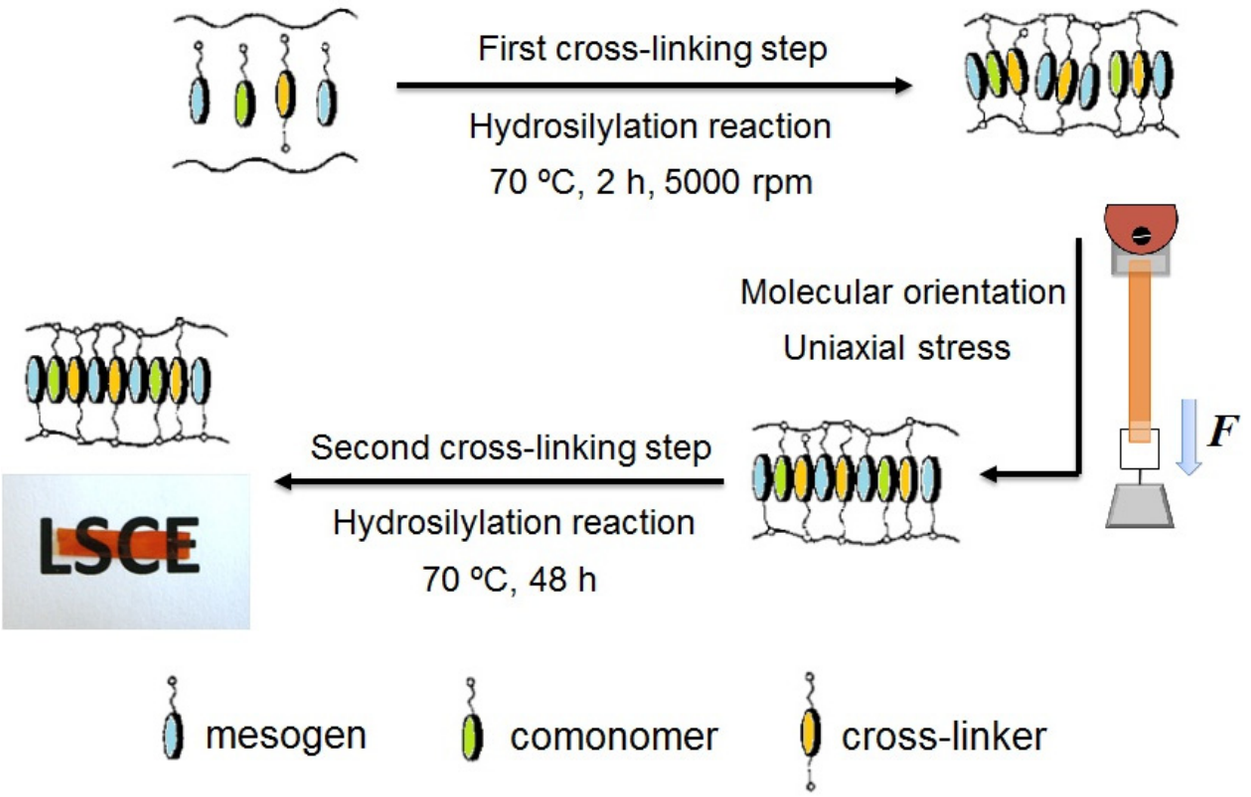

Figure 8. Synthetic methodology in three steps used for preparing photo-active side-chain polysiloxane-based nematic LSCEs.

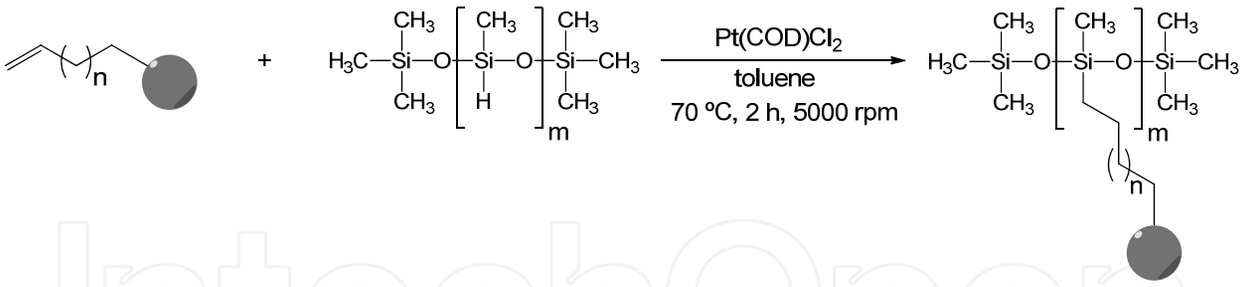

Figure 9. Attachment of an alkene-terminated monomer to the polysiloxane backbone through the Pt-catalysed hydrosilylation reaction. ($Pt(COD)Cl_2$ = dichloro(1,5-cyclooctadiene)platinum(II)).

Figure 10. Qualitative evaluation of the macroscopic orientation of the different directors of the elastomeric sample by means of their optical transparency: monodomain (a), partial monodomain (b) and polydomain (c).

director or vice versa, reorientation of the mesogens can change the shape of the elastomer (see thermo- and opto-mechanical effects in Section 2 of this chapter). In this way, since an LSCE is prepared, its macroscopic dimensions are directly determined by the degree of order created during the second stage of its fabrication. So, the macroscopic orientation of the different directors of the system becomes the key step of the whole synthetic procedure since it will determine the proper actuation of the final material.

In the third stage of the synthesis, the created anisotropy should be fixed by a second cross-linking reaction without removing the applied force. This second hydrosilylation reaction is carried out completely in an oven at 70 °C for 48 h. Afterwards, the LSCE is purified in order to remove both the catalyst and the non-reacted monomers (*ca.* less than 1%) from the network. This cleaning procedure is carried out by a swelling-deswelling process using acetone and hexanes, respectively. Finally, the complete characterisation of the prepared LSCE should be done. The conventional techniques used for characterising nematic LSCEs are briefly described below.

Not only the proper macroscopic orientation but also both the thermal and the mechanical properties of liquid-crystalline elastomers can be studied by means of a wide variety of techniques. Generally, polarised optical microscopy (POM) and X-Ray diffraction (XRD) are used together to get insight into the structure of the mesophase unambiguously but also to evaluate its macroscopic ordering. Moreover, differential scanning calorimetry (DSC) is needed to determine the temperature range of stability of the LC phase. Besides these techniques, additional experiments, such as swelling experiments, are performed on LSCEs to be used further for muscle-like actuation purposes.

The density of cross-linking units present in an LSCE, which is directly related with the mechanical properties of the elastomeric material, can be easily evaluated by means of swelling experiments. Liquid-crystalline elastomers, as a main difference with linear liquid-crystalline polymers and other solids, cannot be dissolved due to the presence of cross-linking points. When an LSCE is immersed in a suitable solvent, it absorbs a large amount of it without dissolving and, as a consequence, it experiments a large deformation producing a small internal stress in the network. Hence, the free energy change that takes place in the elastomer during its swelling process can be separated in two additive contributions, those are, the free energy of mixing, ΔG_{mix}, and the free energy related with the elastic deformation of the network, ΔG_{el}.[40-42]

Traditional swelling experiments are carried out by placing the sample in a vessel containing a suitable solvent (*e.g.* toluene).[43] Then, the system is allowed to reach the thermodynamically equilibrium conditions ($\Delta G_{swelling} = 0$; $\Delta G_{mix} = -\Delta G_{el}$). The swelling parameter, q, is defined as the ratio of volumes of the swollen and original elastomer both measured under thermodynamically equilibrium conditions. Because of the anisotropy of the liquid-crystalline elastomer in its z- direction (**Figure 11**), both x- and y-isotropic dimensions change in the same way but differently from the z- one. Thus, the swelling parameter can be expressed as it is indicated in eq. 1.

$$q = \frac{V}{V_0} = \frac{x \cdot y \cdot z}{x_0 \cdot y_0 \cdot z_0} = \frac{z}{z_0} \cdot \left(\frac{x}{x_0} \right)^2 \quad (1)$$

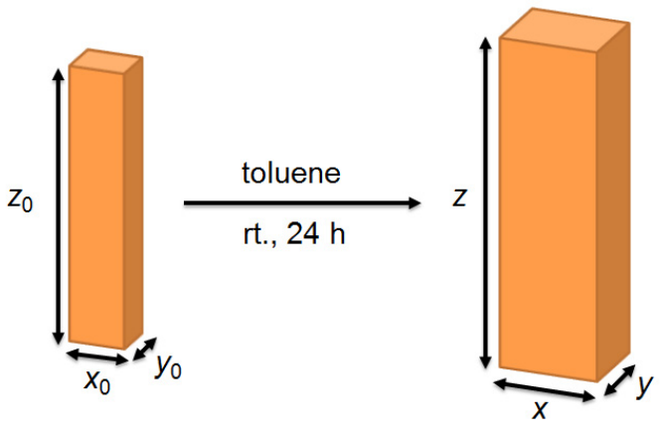

Figure 11. Change in the elastomer volume on reaching thermodynamically equilibrium after swelling.

According to that mentioned above, those samples that contain a high density of cross-linking units will yield a low value of the swelling parameter. However, it is highly remarkable that the magnitude of the swelling parameter depends also greatly on the chemical nature of the cross-linker. In this way, elastomers with more rigid cross-linkers afford lower values of the swelling parameter than those with more flexible ones, although they contain the same density of cross-linking points.[44]

4. Opto-mechanical effect in liquid single crystal elastomers

The macroscopic dimensions of an LSCE are directly related with the degree of order induced during its fabrication. So, any reorientation of the mesogens will lead to changes in the shape of the elastomer. When a photo-active LSCE is illuminated with light of the appropriate wavelength, the azo-chromophore changes its geometry from linear to bent due to its *trans*-to-*cis* photo-isomerisation. This fact produces a microscopic disorganisation of those mesogen molecules that are close to the azo-dye ones producing a decrease in the local order parameter. As a consequence of this molecular disorganisation, a shortening of the LSCE in the director direction is observed (see **Figure 6b**). If the network is fixed by both ends, the system cannot shrink and, as a consequence, the appearance of a retractive force in the elastomer is observed.[38-39]

Opto-mechanical experiments consist in the measurement of the evolution of the internal stress generated inside the LSCE with the time. A typical opto-mechanical experiment for a photo-active liquid single crystal elastomer is shown in **Figure 12**. On turning on the light, the internal stress created in the elastomer, σ, grows until the photo-stationary state is reached. The curve describes a *plateau* which corresponds to the maximum opto-mechanical response produced by the artificial muscle-like actuator, $\Delta\sigma_{max}$. When the irradiation is ceased, the thermal back *cis*-to-*trans* isomerisation of the azo-dye occurs and the stress starts to diminish with the time until the initial stress value is recovered.

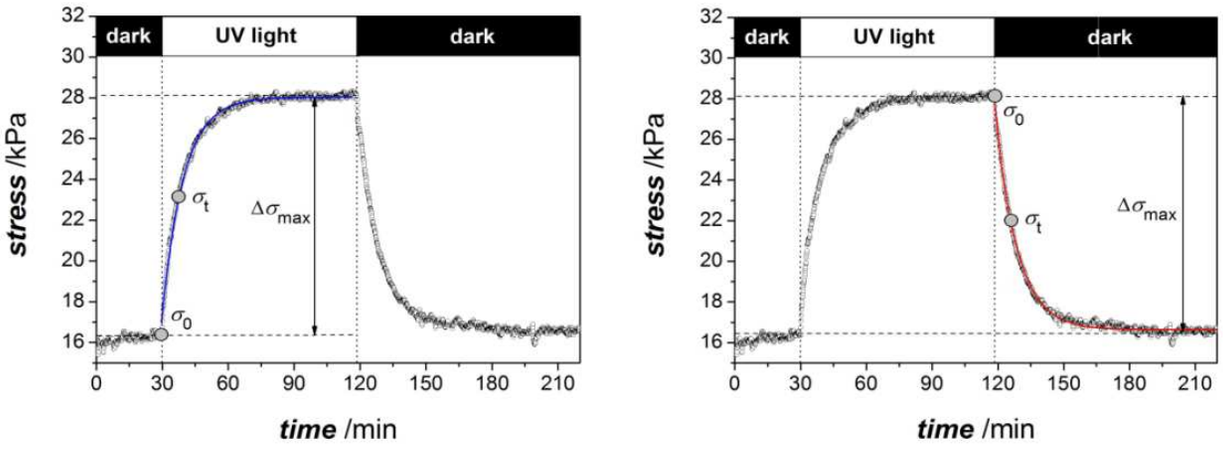

Figure 12. Opto-mechanical experiments: increase of the internal stress generated in the network upon irradiation with UV light (left) and decrease of the stress with the time in the dark at a constant temperature, *T* (right).

Besides the maximum stress that the system is able to generate when UV light falls on it, $\Delta\sigma_{max}$, opto-mechanical experiments allow also determining the time required by the network to produce its maximum mechanical response, τ^{irrad}, and that necessary to recover the initial state thermally, τ^{th}. These three parameters are crucial in the overall performance of LSCEs for artificial muscle-like photo-actuation.

The UV-irradiation process of an LSCE is a bidirectional step, since the *trans*-to-*cis* photo-isomerisation reaction competes with the thermal *cis*-to-*trans* isomerisation simultaneously.

$$trans \underset{k^{th}}{\overset{k^{ph}}{\rightleftharpoons}} cis \tag{2}$$

Both individual isomerisation processes are well known to follow a first order profile for low-molecular weight azoderivatives in isotropic and nematic solution as well as in dense polymer matrixes.[45] Assuming a similar kinetic behaviour for LSCEs, the rate of this process is given by both the disappearance of the *trans* isomer with the time by the photo-induced reaction and its formation through the thermally-activated one (eq. 3).

$$v = -\frac{d[T]}{dt} = k^{ph} \cdot [T] - k^{th} \cdot [C] = k^{ph} \cdot [T] - k^{th} \cdot \left([T]_0 - [T] \right) \tag{3}$$

k^{ph} and k^{th} correspond to the first-order rate constants for the photo-induced *trans*-to-*cis* and the thermal *cis*-to-*trans* isomerisation processes of the elastomeric network, respectively. [*T*] and [*C*] stand for the concentration of *trans* and *cis* isomer at each moment of the reaction, respectively, and $[T]_0$ is the total concentration of azo-dye present in the elastomeric system, that is, the total number of *trans* plus *cis* isomers. $[T]_0$ is a constant value and it is given by the initial composition of the material.

Once integrated the differential equation 3, one gets the time-dependence of the concentration of both isomers *trans* (eq. 4) and *cis* (eq. 5). The curve describing this process is

an exponential growth with an apparent rate constant, k^{irrad}, which is related with the first-order kinetic constants of both processes ($k^{irrad} = k^{ph} + k^{th}$).

$$[T] = [T]_0 \frac{k^{th} + k^{ph} \cdot \exp\left[-(k^{ph} + k^{th}) \cdot t \right]}{k^{th} + k^{ph}} = [T]_0 \frac{k^{th} + k^{ph} \cdot \exp\left[-k^{irrad} \cdot t \right]}{k^{irrad}} \quad (4)$$

$$[C] = [T]_0 \frac{k^{ph}}{k^{th} + k^{ph}} \left(1 - \exp\left[-(k^{ph} + k^{th}) \cdot t \right] \right) = [T]_0 \frac{k^{ph}}{k^{irrad}} \left(1 - \exp\left[-k^{irrad} \cdot t \right] \right) \quad (5)$$

As we mentioned above, the generation of the *cis*-isomer in the LSCE is the responsible of the mechanical stress observed when the sample is UV-irradiated. In fact, the bent *cis* isomer should be considered as an impurity which shifts the critical temperature of the nematic-to-isotropic phase transition of the LSCE (see Section 1 of this Chapter).[38] Hence, equation 5 can be transformed into equation 6 which stands for the variation of the measured internal stress produced by the elastomer shrinking with the time when it is illuminated with UV light.

$$\sigma_t - \sigma_0 = \Delta\sigma_{max} \cdot \left(1 - \exp\left[-k^{irrad} \cdot t \right] \right) \quad (6)$$

On the other hand, the thermal relaxation process of the LSCE is a unidirectional step.

$$\textbf{\textit{cis}} \xrightarrow{k^{th}} \textbf{\textit{trans}} \quad (7)$$

In this case, the rate of the process is given uniquely by the disappearance of the *cis* isomer with the time. The rate equation for this unimolecular first-order reaction is described by equation 8.

$$v = -\frac{d[C]}{dt} = k^{th} \cdot [C] \quad (8)$$

The integration of the differential equation 8 yields the integrated rate equation 9 which describes the evolution of the *cis* isomer concentration with the time during the thermal relaxation of the network. The curve describing this process is an exponential decrease with a first-order rate constant, k^{th}.

$$[C] = [C]_0 \cdot \exp\left(-k^{th} \cdot t \right) \quad (9)$$

In the same manner than for eq. 6, equation 9 can be transformed into eq. 10 which fits for the variation of the measured internal stress in the elastomer with the time when it is kept in the dark at a constant temperature, T:

$$\sigma_t - \sigma_0 = \Delta\sigma_{max} \cdot \exp\left(-k^{th} \cdot t \right) \quad (10)$$

The maximum stress that the system is able to generate upon irradiation, $\Delta\sigma_{max}$, is directly obtained by subtracting the initial stress, σ_0, from the steady-state saturation value reached

under irradiation (see **Figure 12**). Both k^{irrad} and k^{th} are determined by fitting equation 6 and 10 to the experimental data, respectively. The characteristic times for both processes, τ^{irrad} and τ^{th}, are calculated from k^{irrad} and k^{th}, respectively, as $\tau = 1/k$.

The thermal activation parameters, the enthalpy ($\Delta H^{\neq}$) and entropy ($\Delta S^{\neq}$) of activation, can be easily determined by studying the evolution of both isomerisation rate constants as a function of the temperature. This behaviour is well described by means of Eyring's equation (eq. 11).[46-47]

$$\ln\frac{k}{T} = \frac{-\Delta H^{\neq}}{R}\cdot\frac{1}{T} + \ln\frac{k_B}{h} + \frac{\Delta S^{\neq}}{R} \quad (11)$$

R is the universal gas constant (R = 8.314 J·K^{-1}·mol^{-1}), k_B is the Boltzmann's constant (k_B = 1.381 × 10^{-23} J·K^{-1}) and h is the Planck's constant (h = 6.626 × 10^{-34} J·s), respectively.

The characteristic parameters ($\Delta\sigma_{max}$, τ^{irrad} and τ^{th}) for all the artificial muscle-like actuators presented herein have been determined according to the kinetic model described above. The relaxation time registered for the different photo-active LSCEs reported in this chapter ranges from several hours to a few seconds. This fact demonstrates that not only fast-responding artificial muscles but also bistable systems can be obtained easily from polysiloxane-based LSCEs just through the proper substitution of the light-sensitive azo-chromophore.

5. Mechanical efficiency of photo-active liquid single crystal elastomer-based actuators through the variation of the azo-cross-linker flexible spacer

Light-controlled artificial muscle-like actuators based on photo-active polysiloxane LSCEs have been growing interest during the last decade and deeply investigated from both the theoretical and the experimental point of view. As it has been aforementioned, two key parameters are needed to characterise properly the actuation ability of such materials, those are, the maximum mechanical response that they are able to generate by irradiation with light of the appropriate wavelength as well as the time required to produce it and that to recover the initial state further. At the present moment, many efforts are being put forward to improve and optimise both of them.

At this point, we will turn our attention towards the enhancement of the mechanical response produced by those photo-actuators based on polysiloxane azobenzene-containing LSCEs. One of the factors that has been probed to play a clear role on the mechanical response produced by such light-driven actuators is the variation of the photo-active azo-cross-linker spacer length, in other words, the flexible alkyl chain that links the azobenzene core with the main polysiloxane backbone (**Figure 13**).[48]

In order to describe this effect, five different photo-active elastomers containing the nematic mesogen 4-methoxyphenyl-4-(3-butenyloxy)benzoate (**M4OMe**, 90 % mol), the isotropic cross-linker 1,4-di-(10-undecenyloxy)benzene (**V1**, 5 % mol) and one of the light-sensitive

cross-linkers shown in **Figure 13** (**AZOX**, 5 % mol) will be considered (**Figure 14**). All elastomers were prepared and characterised according to that described previously in Section 3 and 4 of this chapter. The photo-active azo-cross-linkers present lateral alkoxyl chains of different lengths, bearing 3, 4, 6, 8 and 11 carbon atoms, n, and thereby producing a total number of methylene units in the flexible spacer, n_{total}, of 6, 8, 12, 16 and 22, respectively. All the systems exhibited a broad enantiotropic nematic phase between their glass transition temperature at T_g = 261-276 K and their nematic-to-isotropic phase transition temperature at $T_{N\text{-}I}$ = 336-342 K ($\Delta H_{N\text{-}I}$ = 1.6-2.1 J·g^{-1}). Table 1 displays the temperature range of stability of the nematic liquid-crystalline phase for each LSCE. Moreover, all of them showed a clear macroscopic orientation of the director as it reveals their orientational order parameter which falls between 0.71 and 0.73. The swelling ratio, q, of the different elastomers ranges from 2.5 to 4.3. According to that discussed in Section 3 of this chapter, the slight differences observed in the swelling parameter for the different systems can be related with the different length of their cross-linker spacer. In this way, elastomer **EAZO3**, which has the most rigid cross-linker, shows the lowest q value (q = 2.5) whereas **EAZO11**, with the most flexible one, exhibits the highest swelling parameter (q = 4.3, Table 1) since it can create bigger empty spaces inside the elastomeric system.

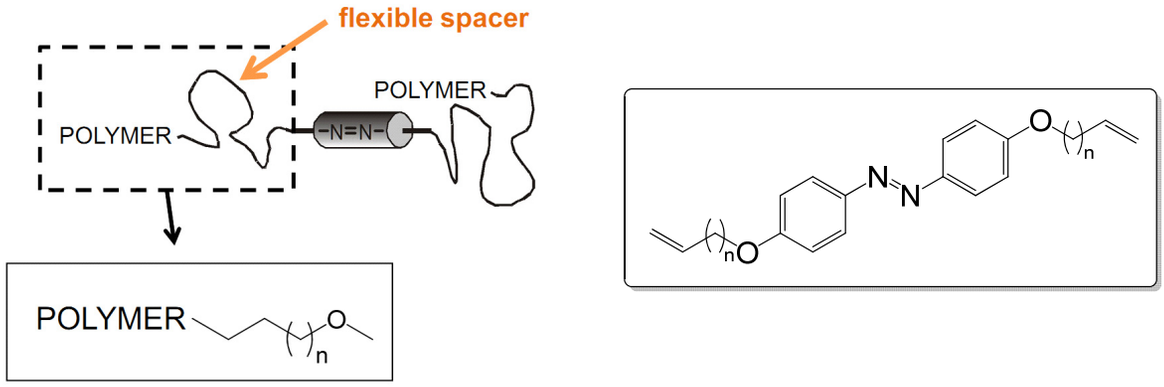

Figure 13. Concept of flexible spacer and general chemical structure of the different photo-active azo cross-linkers used in this study.

Elastomer	S	T_g (K)	$T_{N\text{-}I}$ (K)	$\Delta H_{N\text{-}I}$ (J·g^{-1})	q
EAZO3	0.71	265	336	1.9	2.5
EAZO4	0.73	261	340	2.1	3.0
EAZO6	0.73	264	342	1.6	3.3
EAZO8	0.73	284	348	1.6	3.0
EAZO11	0.72	276	342	1.8	4.3

Table 1. Nematic order parameter, S; glass transition and nematic-to-isotropic phase transition temperatures, T_g and $T_{N\text{-}I}$; nematic-to-isotropic phase transition enthalpy, $\Delta H_{N\text{-}I}$; and swelling parameter, q.

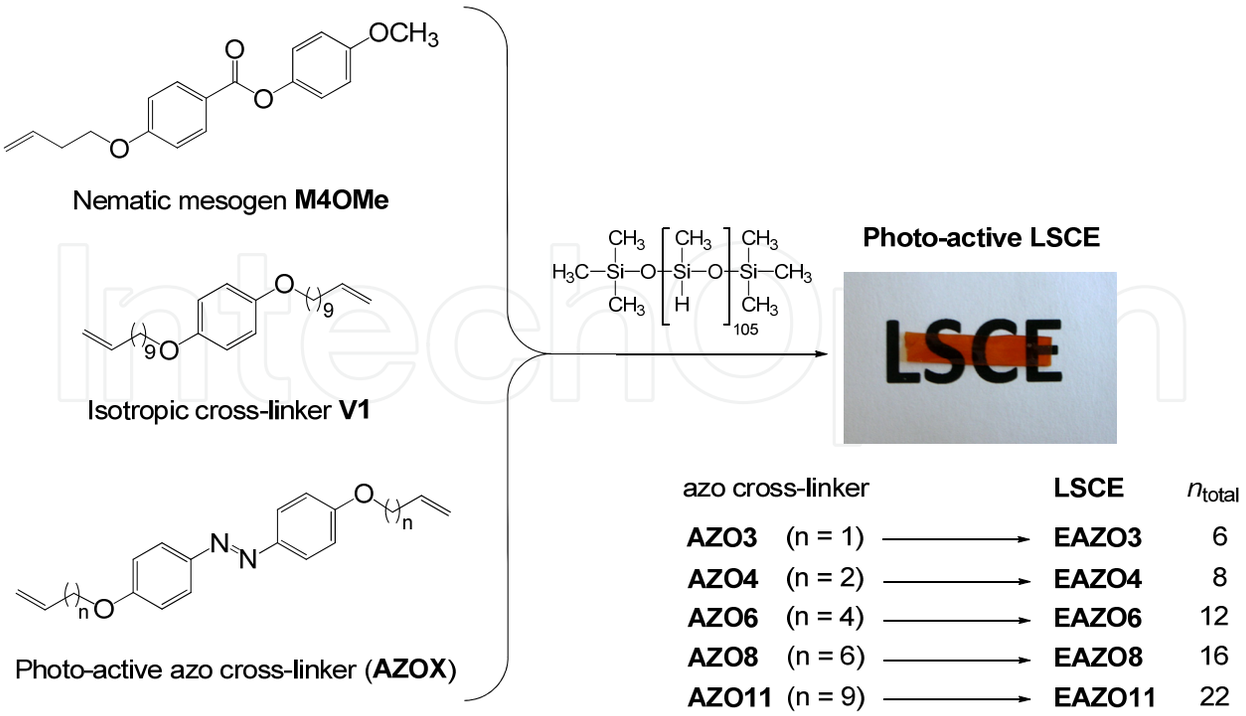

Figure 14. Chemical composition of the different photo-active nematic LSCEs **EAZOX**.

The maximum opto-mechanical response produced by the different LSCEs **EAZOX** under UV-irradiation, $\Delta\sigma_{max}$, depends clearly not only on the number of methylene units of the flexible spacer (**Figure 15**, left) but also on the temperature (**Figure 15**, right). It is highly remarkable that very much efficient light-controlled artificial muscle-like actuators are obtained on using photo-active cross-linkers with long alkoxyl chains in their flexible spacers. Hence, a maximum opto-mechanical response of $\Delta\sigma_{max}$= 19.0 kPa is registered for the LSCE **EAZO11** at 333 K, which bears the longest spacer. Otherwise, a three-fold lower value of $\Delta\sigma_{max}$= 6.4 kPa is obtained for the nematic elastomer **EAZO3** at the same temperature, which contains the shortest one.

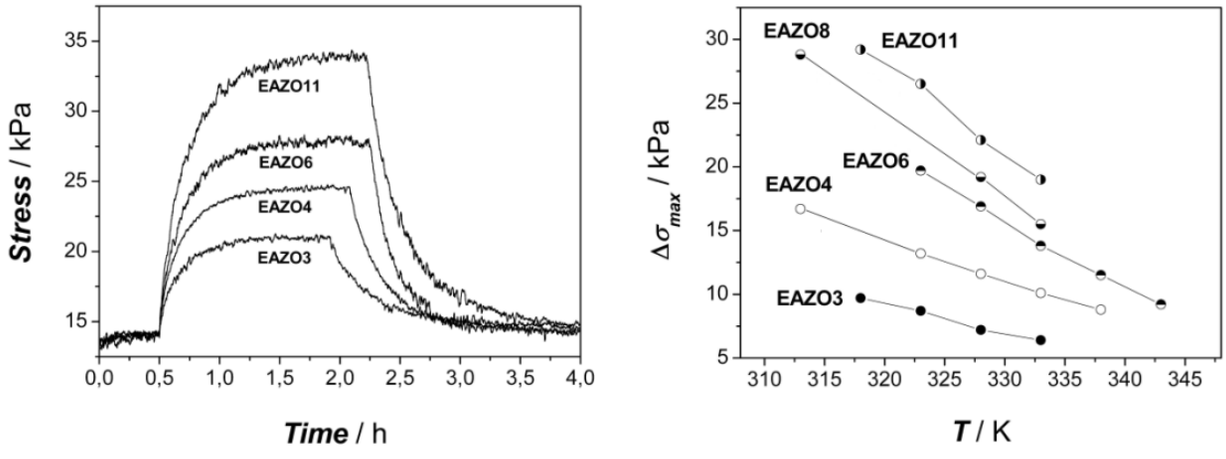

Figure 15. Opto-mechanical experiments for the different nematic liquid single crystal elastomers under irradiation with UV light (λ_{irrad} = 380 nm) at 333 K (left). Evolution of the maximum opto-mechanical response, $\Delta\sigma_{max}$, generated by the different elastomers with the temperature (right).

According to the molecular model presented in **Figure 16**, azo-cross-linkers with long spacers can connect two quite separated points of the main polysiloxane backbone in comparison with their shorter counterparts. As the azo-cross-linker is clamped by both ends, the constraint of the elastomer after the photo-isomerisation to the *cis*-isomer should be greater for those systems which connect two points of the polymeric backbone which are far away separated. Indeed, the cross-linker with the longest spacer experiments the highest opto-mechanical response when the azo moiety adopts its bent geometry.

As a representative example, **Figure 16** shows the calculated distance for the all *trans* conformation of both **AZO3** and **AZO11**, which bear a total number of methylene units in their flexible spacer, n_{total}, of 6 and 22, respectively. For *trans*-**AZO3** and *trans*-**AZO11**, the calculated distance between both terminal carbon atoms are 17.6 and 35.5 Å, while for their corresponding *cis* form, which has a bent shape, it drops until 9.8 and 18.8 Å, respectively. This fact is reflected in a distance change between both terminal carbon atoms that are attached to the main polymeric chain of the network of 7.8 and 16.7 Å, respectively, when the azoderivative is isomerised upon UV-irradiation. Hence, from the calculated distances, it should be expected a greater effect on the macroscopic dimensions of the elastomer when azo-cross-linkers with larger flexible spacers are used. Although the presented model is a qualitative estimation, since the flexible spacer of the azo-cross-linker undergoes a conformational equilibrium, it stands for the different experimental observations.

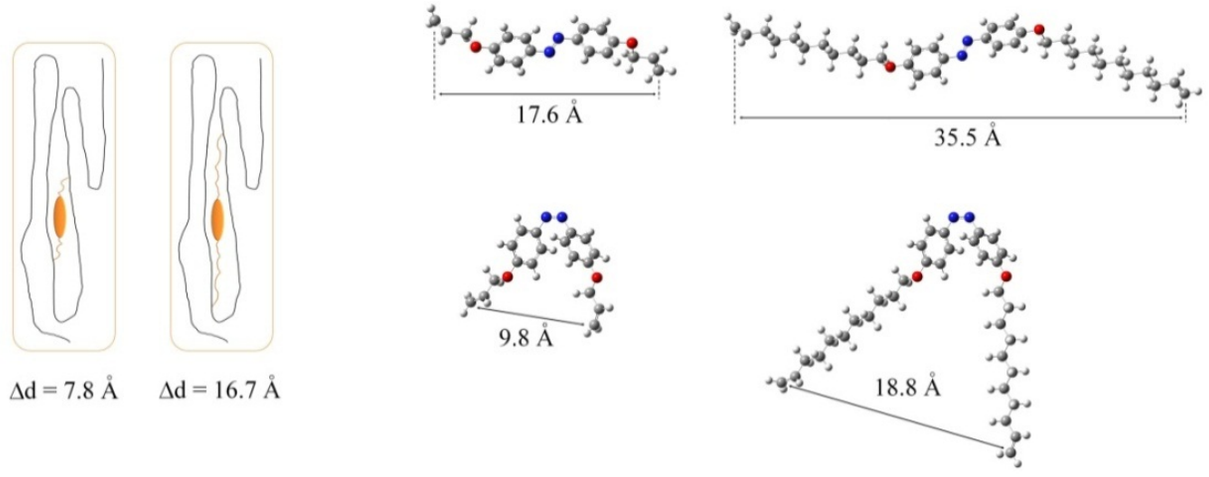

Figure 16. Schematic model of the bonding points of the photo-active azo-cross-linker with the elastomeric network (left). Molecular model for the all *trans* conformation of azo-dyes **AZO3** and **AZO11** and calculated distances between both terminal carbon atoms (right) ($\Delta d = d_{trans} - d_{cis}$).

On the other hand, a marked decrease of the opto-mechanical response of the artificial muscle-like actuator on rising the temperature is detected. This phenomenon is well understood since the thermal back isomerisation process, which competes with the *trans*-to-*cis* photo-isomerisation reaction, takes place faster on increasing the temperature and, consequently, the *cis* isomer concentration at the photo-stationary state, which is the responsible of the observed mechanical response, is lower at higher temperatures.

Moreover, the maximum opto-mechanical response at a determined temperature, T, shows a clear dependence on the total methylene units of the cross-linker spacer, n_{total} ($n_{total} = 2n + 2$, where n is the number of methylene units of the alkoxyl chain). A growing exponential behaviour tending to a *plateau* for a long spacer length is observed at each temperature. It can be nicely seen from **Figure 17**, that there is a threshold length value for the flexible spacer from which the mechanical response of the system is not enhanced anymore. The threshold spacer length value for the selected architecture of the photo-active azoderivative corresponds to *ca.* $n_{total} \approx 30$ methylene units, that is, 15 carbon atoms in each alkoxyl chain of the flexible spacer.

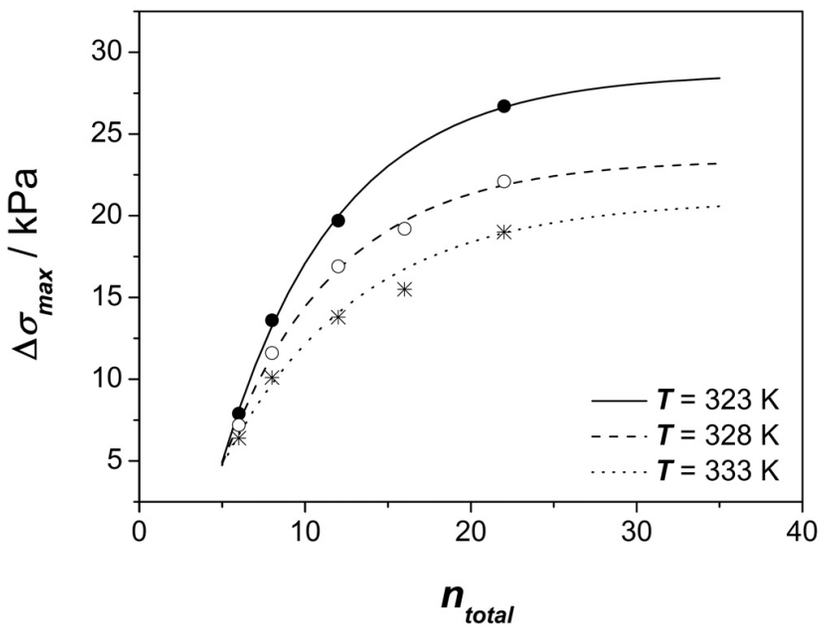

Figure 17. Evolution of the maximum opto-mechanical response, $\Delta\sigma_{max}$, with the total number of methylene units in the spacer, n_{total}, at different temperatures.

The result displayed in **Figure 17** evidences that there is a maximum opto-mechanical response for each type of azo-cross-linker used. In this case, responses up to 30 kPa can be obtained using 4,4'-dialkoxysubstituted azo-dyes as photo-active cross-linkers at 323 K. Considering a linear relationship between $\Delta\sigma_{max}$ and T (see **Figure 15**, right), it can be concluded that this type of azo-cross-linkers can afford responses up to 60 kPa at room temperature.

The analysis of the characteristic times found for both the whole UV-irradiation (τ^{irrad}) and the thermal relaxation (τ^{th}) process when the azo-dye is incorporated as a cross-linker in the nematic LSCE yields that the rate of both processes is independent of the length of the azo-cross-linker spacer. The relaxation time for the irradiation process ranges from 15 to 21 minutes at 323 K. For the reverse process, the thermal isomerisation in the dark, relaxation times ranging from 29 to 35 minutes were registered for all the LSCEs at 323 K, except for **EAZO3** which showed a slightly higher value of 45 minutes, probably related with the lower flexibility of the azo-cross-linker (**Table 2**). The thermal *cis*-to-*trans* isomerisation of

the azo-dye takes place faster inside the nematic LSCE than in isotropic media, but it is similar to that obtained in low molar mass liquid crystals. This fact evidences that the kinetic acceleration of the thermal *cis*-to-*trans* isomerisation of the azo-dye in the LSCE is mainly due to the presence of the nematic mean field in the network.[49-51]

Elastomer	323 K		328 K		333 K	
	τ^{irrad}	τ^{th}	τ^{irrad}	τ^{th}	τ^{irrad}	τ^{th}
EAZO3	19.8	44.1	15.7	30.0	12.4	20.0
EAZO4	18.3	34.5	14.1	22.5	10.8	15.9
EAZO6	15.3	29.0	12.8	20.0	10.7	14.7
EAZO8	18.5	30.3	15.1	20.2	12.8	14.4
EAZO11	20.5	33.5	17.3	23.8	14.4	16.4

Table 2. Relaxation time for the *trans* isomer under irradiation with UV light, τ^{irrad}, and for the *cis* isomer on heating in the dark, τ^{th} at different temperatures. All values are given in minutes.

Although all the photo-active LSCEs presented till this moment are mechanically efficient, they need several hours to reach their maximum mechanical response and also to relax back to the initial state.[37,38,48] Hence, the time required by the network to recover its initial dimensions is also another crucial parameter to consider for obtaining functional artificial muscle-like actuators. Likewise, our discussion will be focused in the next section on presenting different strategies to get photo-active artificial muscle-like actuators with a low thermal relaxation time.

6. Response time of artificial muscle-like actuators by using fast thermally-isomerising azoderivatives

While the *trans*-to-*cis* photo-isomerisation can be easily accelerated either by using more powerful light sources or the appropriate modification of the azobenzene core, the thermal *cis*-to-*trans* back reaction depends mainly not only on the chemical functionalization of the azo-dye but also on the environment where the azo-chromophore is located. Hence, it is essential for getting fast azobenzene-based artificial muscle-like actuators that the return to the thermodynamically stable *trans* form of the azo-chromophore in the dark elapses as fast as possible.

Only two examples of dye-doped polysiloxane-based photo-active nematic LSCEs with a fast isomerisation rate have been published so far. These systems use the well-known push-pull azo-dyes 4-amino- and 4-*N*,*N*-dimethylamino-4′-nitroazobenzene as photo-active molecules, which are doped into host elastomeric networks but not covalently bonded to the polymeric structure[52,53]; this fact decreases the stability of the final photo-actuator. Besides those azoderivatives which bear a push-pull configuration, azophenols are also endowed with a very rapid thermal *cis*-to-*trans* isomerisation process since they are capable to establish azo-hydrazone tautomeric equilibria which allows their thermal back reaction to proceed through

the rotational isomerisation mechanism. Hence, these two type of azoderivatives are valuable photo-active molecules to be introduced as covalently bonded comonomers in LSCE to obtain stable and fast responding photo-sensitive elastomeric materials.

6.1. Artificial muscle-like actuators using push-pull azoderivatives as chromophores

Since an azo-dye is introduced into a polymer, the polymer backbone undergoes different motions when the thermal relaxation of the azoderivative occurs. These motions may modify the kinetic parameters of the *cis*-to-*trans* isomerisation of the azo chromophore. In this way, structural factors such as chain flexibility and chain conformation play an important role on the rate of the thermal isomerisation process of the chromophore.[45,54,55] Moreover, very different kinetic behaviour should be expected when the azo-dye is bonded to the polymer backbone than when it is just dissolved in the host polymer matrix as a doped guest. This effect has been already detected in LSCEs that contain the push-pull azo-dyes 4-(5-hexenyloxy)-4'-nitroazobenzene and 4-(5-hexenyloxy)-4′-methoxy-2′-nitro-azobenzene introduced as side-chain covalently-bonded photo-active moieties (**Figure 18**).[56]

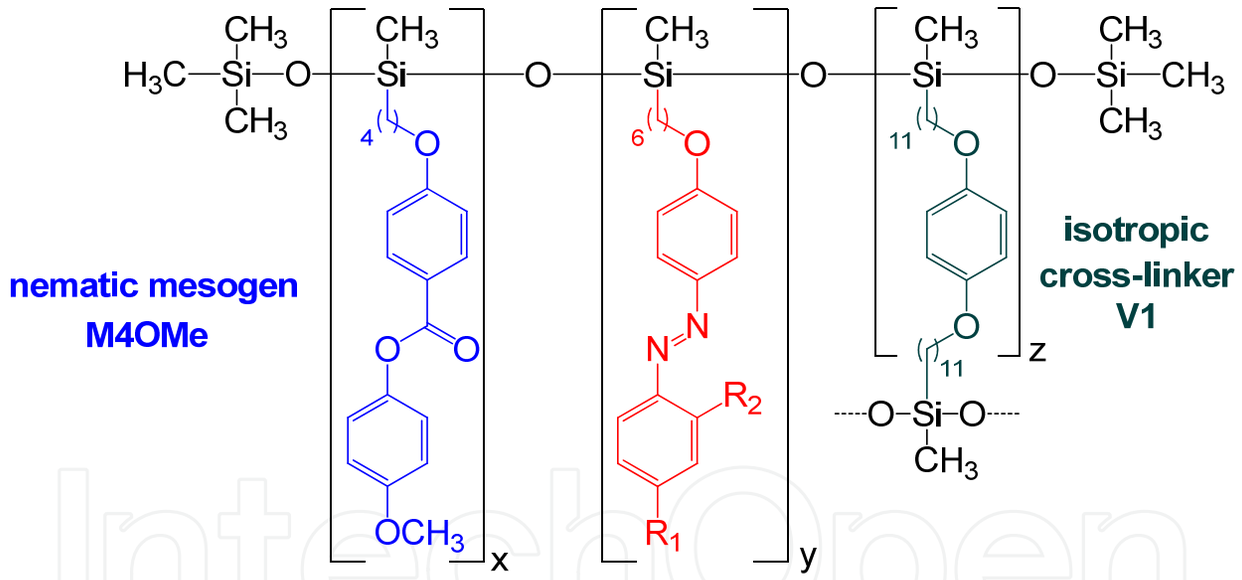

E*p*NO₂ $R_1 = -NO_2$; $R_2 = -H$ (x : y : z 0.85 : 0.05 : 0.10)

E*o*NO₂ $R_1 = -OCH_3$; $R_2 = -NO_2$ (x : y : z 0.85 : 0.05 : 0.10)

Figure 18. Chemical composition of the photo-active nematic LSCEs **E*p*NO₂** and **E*o*NO₂**.

For describing this effect, two nematic LSCEs **E*p*NO₂** and **E*o*NO₂** will be considered being composed by the nematogen **M4OMe** (85 % mol), the photoactive co-monomer (**AZO*p*NO₂** or

AZO*o*NO2, respectively, 5 % mol) and the isotropic cross-linking agent **V1** (10 % mol) as it is shown in **Figure 18**. Both elastomers, **E*p*NO2** and **E*o*NO2**, which differ only in the placement of the nitro- electron-withdrawing group, showed a broad enantiotropic nematic phase between their glass transition temperature at T_g = 276-277 K and their nematic-to-isotropic phase transition temperature at $T_{N\text{-}I}$ = 331-332 K ($\Delta H_{N\text{-}I}$ = 1.3-1.7 J·g^{-1}), respectively. Completely transparent monodomain nematic samples were obtained for both elastomers exhibiting orientational order parameters of 0.75 and 0.76 for **E*o*NO2** and **E*p*NO2**, respectively.

The determination of the thermal *cis*-to-*trans* isomerisation rate of both azo-dyes acting as covalently-bonded co-monomers in the nematic LSCE by means of opto-mechanical experiments yielded relaxation times for *cis*-**AZO*p*NO2** and *cis*-**AZOoNO2** of 4 and 3 seconds, respectively, at 298 K. The impressive acceleration of the kinetics of the thermal *cis*-to-*trans* isomerisation of both nitro-substituted azoderivatives in the LSCE is highly remarkable. The process was found to be more than 10^3 times faster in the LSCE, in which the azo-dye is chemically bonded to the polymer backbone, than that observed in isotropic solvents (between 16 and 92 min.), and about 10^2 times quicker than the one shown as a guest chromophore doped in a low molar mass nematic liquid crystal (6-7 min.). This acceleration is associated to the covalent attachment of the push-pull azoderivative to a nematic polymer backbone which possesses an anisotropic chain conformation.[56]

The great acceleration exhibited by these nitro-substituted azo-dyes when they are chemically bonded into nematic LSCEs has been already exploited for the preparation of fast photo-active artificial muscle-like actuators. The maximum opto-mechanical response generated by the elastomer **E*p*NO2** was of $\Delta\sigma_{max}$ = 1.4 kPa, while a lower value of 0.7 kPa was obtained for the LSCE **E*o*NO2** (**Figure 19**). The fast thermal relaxation of these systems is the responsible of the low internal stress generated in both elastomers due to the low presence of *cis* isomer in the photo-equilibrium state. The slightly faster thermal isomerisation for **E*o*NO2** accounts for the lower mechanical response produced by this network. Both LSCEs exhibit a reversible behaviour in the time scale of seconds at room temperature, that is, relaxation times of 2-4 s for the whole irradiation process with blue light and of 3-4 s for the *cis*-to-*trans* thermal relaxation in the dark for **E*o*NO2** and **E*p*NO2**, respectively.

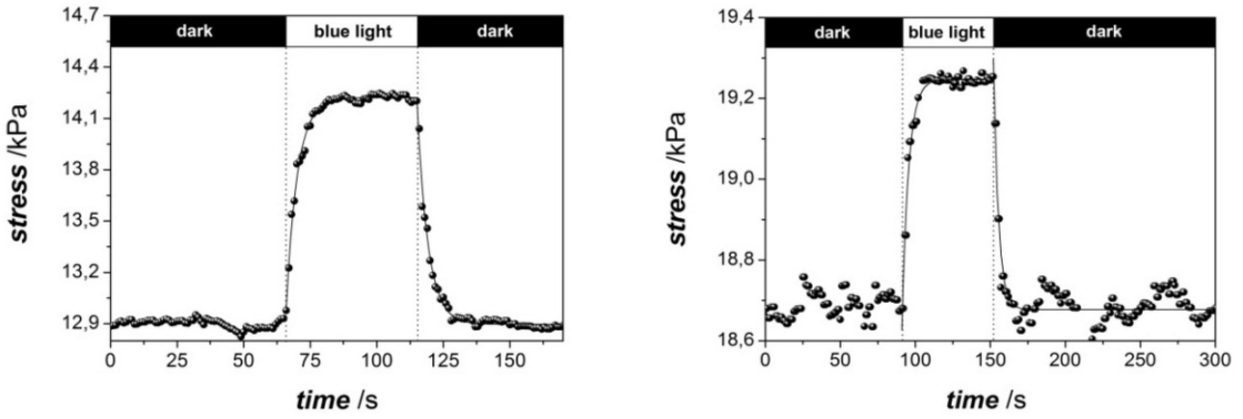

Figure 19. Opto-mechanical experiments for both nematic elastomers **E*p*NO2** (left) and **E*o*NO2** (right) at 298 K (irradiation of the networks was performed with blue light, λ_{irrad} = 450 nm).

6.2. Artificial muscle-like actuators based on azophenol derivatives exhibiting azo-hydrazone taumeric equilibrium

A second strategy to decrease the response time of the artificial muscle-like actuators implies the use of azophenols as photo-active moieties. Azophenols are promising chromophores for designing fast-responding artificial muscle-like actuators since they are endowed with a rapid thermal isomerisation process at room temperature, with relaxation times ranging from 6 ms to 300 ms in polar protic solvents depending on the position of the phenol groups.[57] But, the main drawback is that hydroxyazobenzenes show a fast thermal isomerisation rate only when they are dissolved in polar protic solvents.

A successful strategy to transfer this fast thermal isomerisation to solid elastomeric materials consists in the preparation of a co-elastomer which contains a nematic mesogenic monomer (**M4OMe**) and the photo-active hydroxyazoderivative (**AZO-OH**). The liquid-crystalline co-elastomer obtained contains only a small proportion of the azo moiety (5% mol) in order to not overly disrupt the nematic order of the elastomer. However, in that system, the azo-dye concentration is high enough for hydrogen bonding being established between the hydroxyazobenzene monomers without niether losing the liquid-crystalline properties of the nematic system nor diminishing the temperature range where the nematic phase exists. As a result of this interaction, the resulting LSCE exhibits an isomerisation rate as fast as that of the azo-monomer dissolved in a protic isotropic solvent.[58]

Two different liquid single crystal elastomers will be presented, **EAZO-Ac** and **EAZO-OH**, in order to describe properly the influence of the phenolic group in the opto-mechanical properties of the final photo-actuator (**Figure 20**). The uniaxially oriented acetylated elastomer **EAZO-Ac** was prepared following the well-known spin-casting technique commented above. Elastomer **EAZO-OH** was prepared from **EAZO-Ac** in order to assure an identical composition in both systems. For preparing elastomer **EAZO-OH**, the acetylated elastomer **EAZO-Ac** is swollen in a mixture of CH_2Cl_2 and MeOH (2:1 v/v) with one drop of acetyl chloride at room temperature for 2 days. Acetyl chloride enters the network by diffusion producing a mild and chemoselective cleavage of the ester group of the acetylated side-chain group, **AZO-Ac**, without hydrolysing the other ester group placed in the mesogen.

The characterization of both LSCEs was carried out by using the standard techniques (see Section 3 of this chapter). DSC experiments showed that both elastomers, **EAZO-Ac** and **EAZO-OH**, exhibited a broad enantiotropic nematic phase between their glass transition temperature at T_g = 277-278 K (ΔC_p = 0.3 J·g^{-1}·K^{-1}) and their nematic-to-isotropic phase transition temperature at $T_{N\text{-}I}$ = 335-336 K ($\Delta H_{N\text{-}I}$ = 1.6-1.8 J·g^{-1}), respectively. X-Ray scattering experiments clearly indicate that no change in the degree of order of the LSCE occurred during the cleavage reaction since very close orientational order parameters were obtained for both **EAZO-Ac** and **EAZO-OH** (0.71 and 0.69, respectively). Interestingly, the swelling ratio, q, was determined to be 5.0 and 3.3 for **EAZO-Ac** and **EAZO-OH**, respectively. The lower q value found for **EAZO-OH** evidenced that hydrogen bonding is established between the phenol groups of the azo-dyes in the LSCE acting as additional cross-linking units.

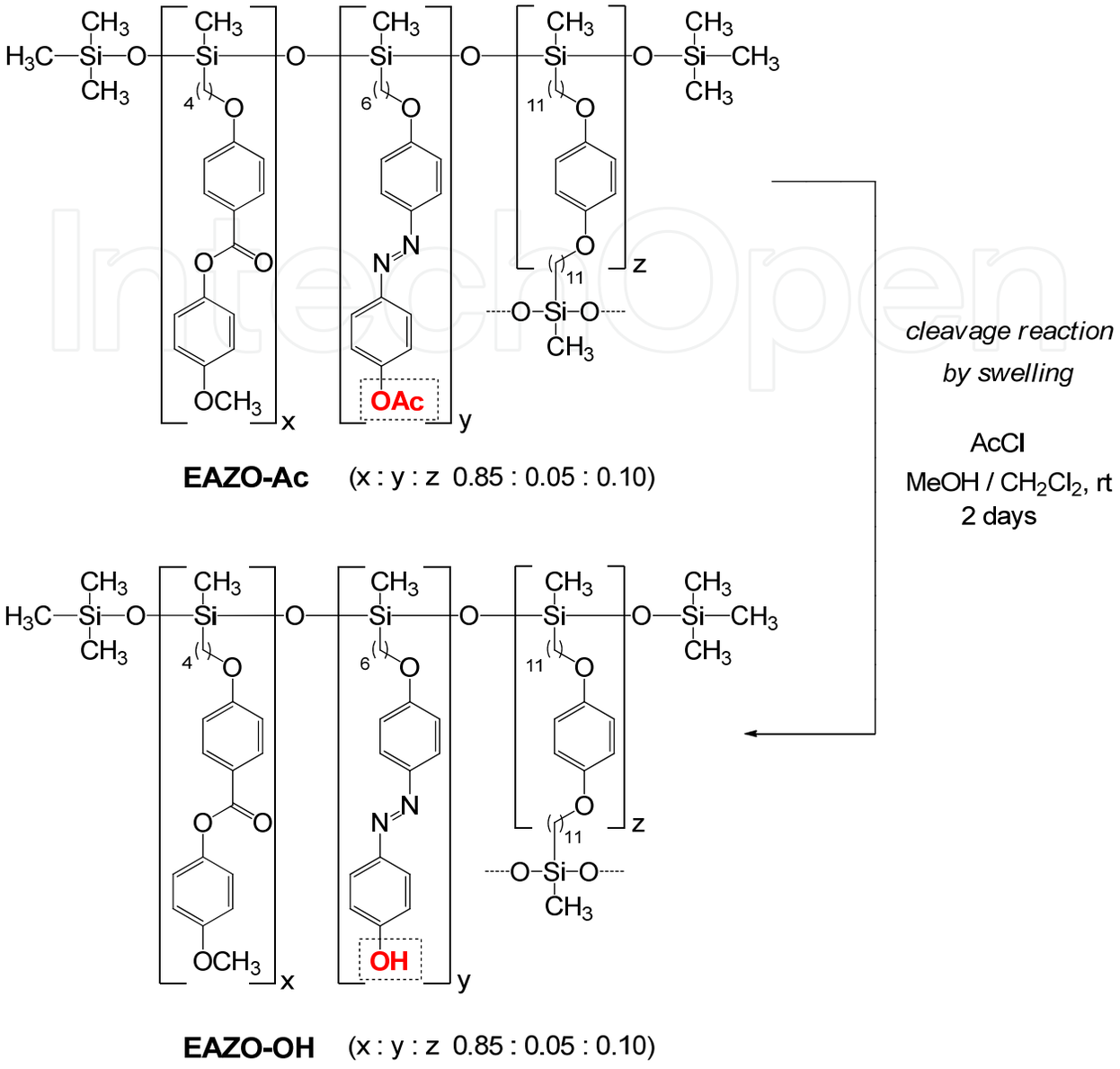

Figure 20. Chemical composition of **EAZO-Ac** and **EAZO-OH** and synthetic concept for the photo-active nematic LSCE **EAZO-OH**.

The analysis of the mechanical response generated by both elastomers as well as their relaxation time by means of opto-mechanical experiments evidenced that both LSCEs, **EAZO-Ac** and **EAZO-OH**, can act as light-controlled actuators when they are irradiated with UV light (λ_{irrad} = 380 nm). **Figure 21** shows the evolution of the internal stress generated inside both LSCEs, **EAZO-Ac** and **EAZO-OH**, with the time at 323 and 298 K, respectively. **EAZO-Ac** produced a maximum opto-mechanical response of $\Delta\sigma_{max}$ = 15 kPa at 323 K (**Figure 21a**). The opto-mechanical response of **EAZO-Ac** was enhanced to *ca.* $\Delta\sigma_{max}$ = 30 kPa on dropping the temperature down to at 313 K (**Figure 22**). When the same experiment is carried out at 298 K for the elastomer **EAZO-OH**, a lower maximum opto-mechanical response of $\Delta\sigma_{max}$ = 0.6 kPa is obtained (**Figure 21b**). Once more, similar results than those aforementioned are obtained. On comparing the non push-pull systems shown in Section 5

with those containing push-pull azoderivatives, which have been presented in Section 6.1, it is clearly seen that the mechanical efficiency, expressed in terms of $\Delta\sigma_{max}$, is greater in the former (up to 60 kPa at 298 K), that is, for those azo-dyes that undergo their thermal *cis*-to-*trans* isomerisation through the inversional mechanism. Otherwise, those azocompounds that isomerises by means of the rotational pathway, those are, push-pull azo-dyes and azophenols, show lower mechanical efficiencies around 0.6 - 1.4 kPa at room temperature.

Besides, the nematic liquid-crystalline elastomer **EAZO-Ac**, which contains the azo-chromophore as a side-chain monomer, is less effective ($\Delta\sigma_{max}$ = 15 kPa at 323 K) than those elastomers **EAZOX**, where the azo-dye is introduced as a photo-active cross-linker in the elastomeric network ($\Delta\sigma_{max}$ = 30 kPa at 323 K).

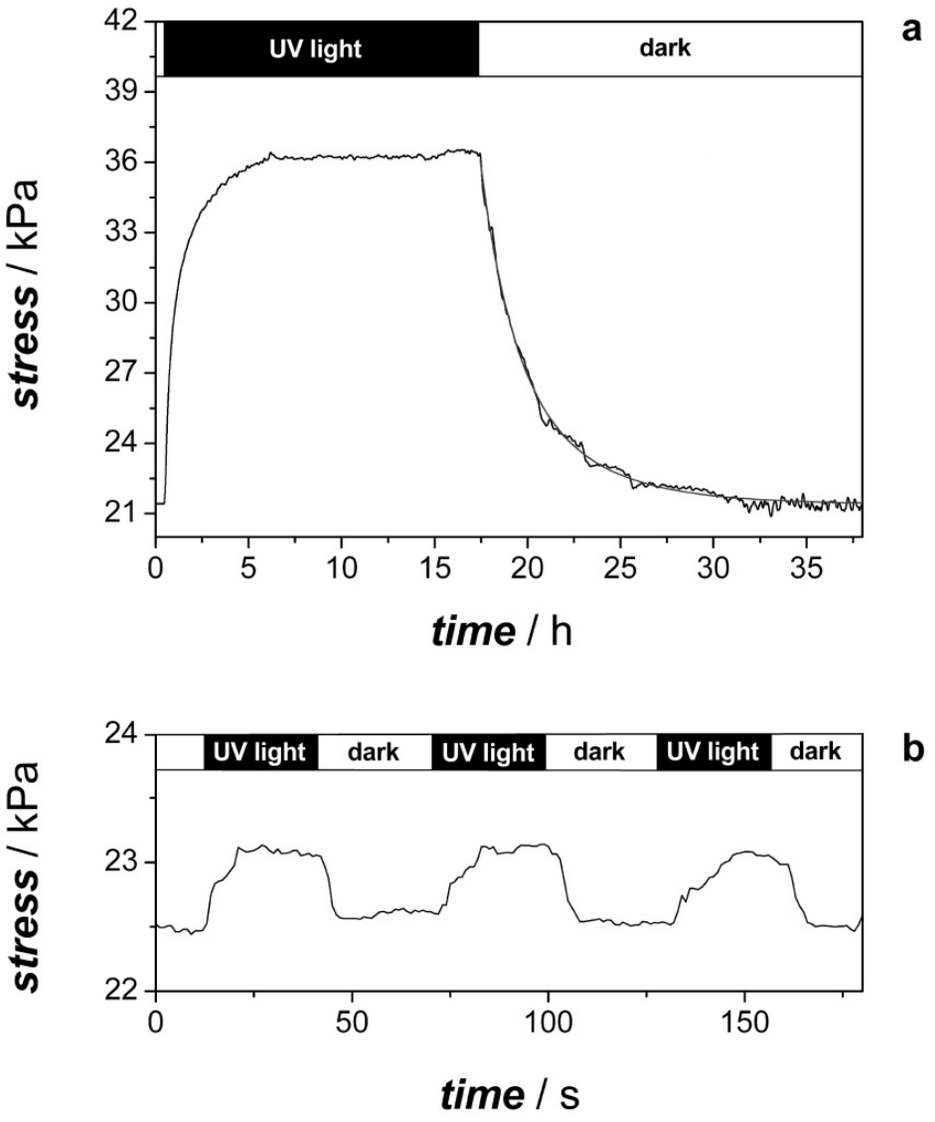

Figure 21. (a) Opto-mechanical experiment for the nematic LSCE **EAZO-Ac** at 323 K.(b) Opto-mechanical experiment for the nematic LSCE **EAZO-OH** at 298 K (λ_{irrad} = 380 nm).

EAZO-Ac exhibits a relaxation time for its thermal back reaction of τ^{th} = 21.3 h at room temperature, which was determined by extrapollation of the corresponding Eyring's plot

(**Figure 23**). Opto-mechanical experiments also reveal a completely different kinetic behaviour between both photo-actuators. While **EAZO-Ac** presents a relaxation time of almost 1 day, **EAZO-OH** gives a value of only 1 s at room temperature. The fast thermal relaxation exhibited by **EAZO-OH** evidences clearly the establishment of hydrogen bonding between the different phenol groups due to their spatial proximity within the elastomeric network. This interaction indicates that the azo-dye isomerisation takes place through the rotational mechanism as it has been described for other azophenol derivatives.[57]

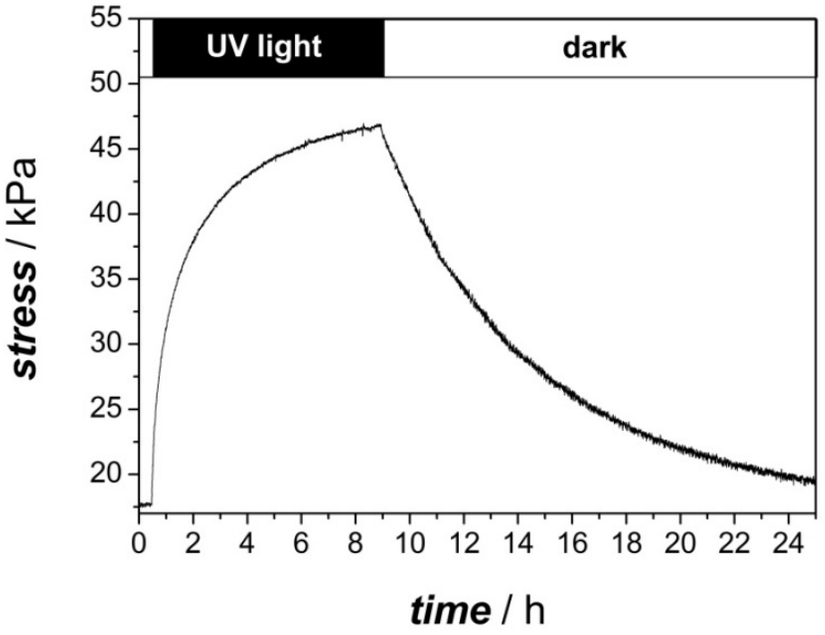

Figure 22. Opto-mechanical experiment for the nematic LSCE **EAZO-Ac** at 313 K (λ_{irrad} = 380 nm).

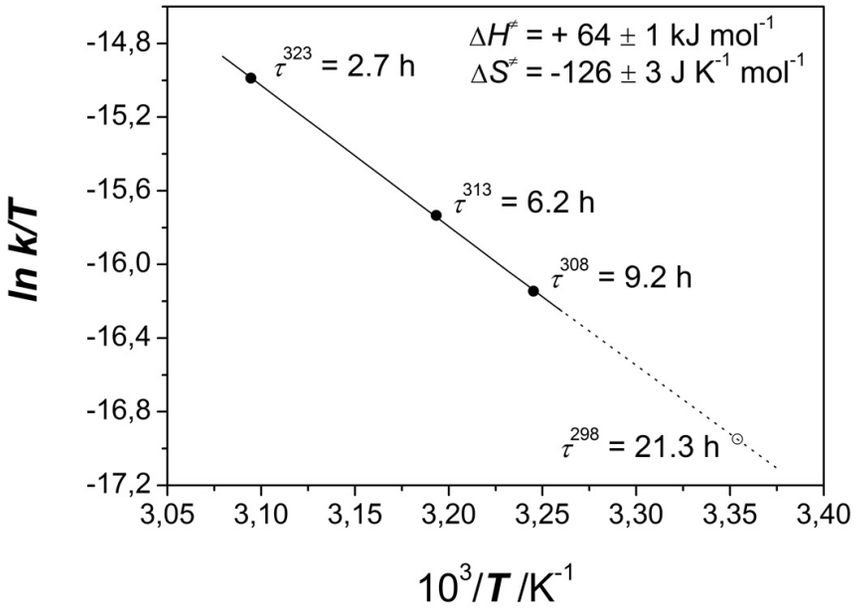

Figure 23. Eyring's plot for the thermal *cis*-to-*trans* isomerisation of **EAZO-Ac**.

The low mechanical response registered for the free-phenol-containing elastomer **EAZO-OH** in comparison with that of **EAZO-Ac** is associated to the low proportion of *cis* isomer present when **EAZO-OH** reaches its photo-equilibrium state at 298 K, as it has been commented above for the nitro-substituted azobenzene-containing elastomers **E*p*NO$_2$** and **E*o*NO$_2$** (see above). Similarly, the slower thermal relaxation of **EAZO-Ac** at 313 K than at 323 K makes the photo-equilibrium state richer in *cis* isomer in the former. This fact accounts for the higher opto-mechanical response exhibited by **EAZO-Ac** at 313 K.

7. Conclusion

Photo-active liquid single crystal elastomers (LSCEs) are valuable materials for artificial muscle-like applications since their macroscopic dimensions can be easily changed by applying light, an environmentally-friendy energy which can be wireless applied to the material. Those actuators based on the azobenzene chromophore are the most commonly used since it presents a clean and totally reversible isomerisation process.

Two different key parameters are crucial for characterising properly the artificial muscle-like actuation of such materials, those are, the maximum mechanical response that they are able to generate by irradiation with light of the appropriate wavelength as well as the time required to produce it and that to recover the initial state further.

The use of non-push-pull azoderivatives, which thermally-isomerise through the inversional mechanism, both as light-sensitive cross-linkers and as side-chain pendant groups in polysiloxane nematic LSCEs produces high mechanically-efficient artificial muscle-like actuators. However, those actuators that bear the photo-active azo-dye as a cross-linker exhibit the highest mechanical efficiency. In such materials, the opto-mechanical response produced by the artificial muscle increases greatly by using larger flexible spacers on the photo-active cross-linker. For 4,4'-dialkoxysubstituted azobenzenes, there is a maximum spacer length, n_{th} ~30, above which the opto-mechanical response of the network reaches a constant value and it is not enhanced anymore. Nevertheless, the relaxation time of the photo-actuator remains unaltered on varying the cross-linker spacer length. Hence, such materials can be used as bistable artificial muscles.

On the other hand, the introduction of both alkoxynitro-substituted azobenzenes and azophenols, which isomerise by means of the rotational pathway, yield fast-responding artificial muscle-like actuators. Indeed these two different types of fast-isomerising azoderivatives have been successfully used as covalently-bonded side-chain chromophores in nematic LSCEs. Alkoxynitro-substituted azobenzenes accelerate up to 10^3 times their thermal *cis*-to-*trans* isomerisation kinetics in isotropic media when they are attached in LSCEs. This rapid thermal isomerisation allows their use as chromophores to get stable and fast artificial muscle-like actuators working in time scale of 1-3 seconds.

Besides, the thermal *cis*-to-*trans* isomerisation process of azophenols depends strongly on the proticity of the environment where they are placed. In this way, their thermal isomerisation rate is accelerated up to 10^4 times if ethanol is used instead of toluene. The fast

isomerisation rate exhibited by these azo-dyes in ethanol has been successfully transferred to polymeric and elastomeric materials, where no solvent is present, due to the hydrogen bonding established between the side-chain azophenol monomers. Similar fast and stable artificial muscle-like actuators than those based on alkoxy-nitro-substituted azobenzenes have been described.

Author details

Jaume Garcia-Amorós and Dolores Velasco
Grup de Materials Orgànics, Institut de Nanociència i Nanotecnologia (IN²UB), Departament de Química Orgànica, Universitat de Barcelona, Barcelona, Spain

Acknowledgement

Financial support from the European project: "*Functional Liquid-Crystalline Elastomers*" (FULCE-HPRN-CT-2002-00169) and from the *Ministerio de Ciencia e Innovación* (CTQ-2009-13797) is gratefully acknowledged. The authors thank Prof. Dr. Heino Finkelmann for its continuous support and helpful discussions.

8. References

[1] F. Reinitzer, *Monatsh. Chem.*, 1998, 9, 421 (Translation in English: *Liq. Cryst.* 1989, 5, 7).
[2] M. Schadt, *Appl. Phys. Lett*., 1971, 18, 127.
[3] H. Iwai, J. Fukasawa and T. Suzuki, *International Journal of Cosmetic Science*, 1998, 20, 87
[4] M. Shlens, M. R. Stoltz and A. Benjamin, *West J. Med.*, 1975, 122, 367.
[5] J. Stasiek, A. Stasiek, M. Jewartowski and M. W. Collins, *Optics & Laser Technology*, 2006, 38, 243.
[6] Y. Yu and T. Ikeda, *Macromol. Chem. Phys.*, 2005, 206, 1705.
[7] T. Mirfakhrai, J. D. W. Madden and R. H. Baughman, *Materials Today*, 2007, 10, 30.
[8] Y. Ishida, Y. Kai, S. Kato, A. Misawa, S. Amano, Y. Matsuoka and K. Saigo, *Angew. Chem. Int. Ed.*, 2008, 47, 8241.
[9] J. W. Goodby and G. Gray, *Handbook of Liquid Crystals*; Wiley-VCH: New York, Weinheim, 1998, 1, 17.
[10] H. Finkelmann in *Thermotropic Liquid Crystals*; John Wiley & Sons, UK, 1987.
[11] H. Finkelmann, H. Ringsdorf and J. H. Wendorff, *Makromol. Chem.*, 1978, 179, 273.
[12] P. J. Collings and M. Hird, *Introduction to liquid crystals: chemistry and physics*; Taylor and Francis Ltd, Bristol, 1997.
[13] P. J. Collings, *Liquid crystals. Nature's delicate phase of matter*; Princeton University Press, New Jersey, 2002.
[14] H. Rau in *Photochemistry and photophysics*; CRC Press Boca Raton FL, 1990.
[15] C. H. Legge and G. R. Mitchell, *J. Phys. D: Appl. Phys.*, 1992, 25, 492.
[16] S. K. Prasad, G. G. Nair, K. L. Sandhya and D. S. S. Rao, *Current Science*, 2004, 86, 815.
[17] Y. Yu and T. Ikeda, *J. Photochem. Photobiol. C: Photochem. Rev.*, 2004, 5, 247.

[18] J. H. Sung, S. Hirano, O. Tsutsumi, A. Kanazawa, T. Shiono and T. Ikeda, *Chem. Mater.*, 2002, 14, 385.
[19] T. Ikeda, J.-I. Mamiya and Y. Yu, *Angew. Chem. Int. Ed.*, 2007, 46, 506.
[20] C. J. Barrett, J.-I. Mamiya, K. G. Yager and T. Ikeda, *Soft Matter*, 2007, 3, 1249.
[21] H. Yu and T. Ikeda, *Adv. Mater.*, 2011, 23, 2149.
[22] T. Ikeda and T. Ube, *Mater. Today*, 2011, 14, 480.
[23] Y. Yu, M. Nakano and T. Ikeda, *Nature*, 2003, 425, 145.
[24] H. Jiang, S. Kelch and A. Lendlein, *Adv. Mater.*, 2006, 18, 1471.
[25] R. Yin, W. Xu, M. Kondo, C.-C. Yen, J.-I. Mamiya, T. Ikeda and Y. Yu, *J. Mater. Chem.*, 2009, 19, 3141
[26] M. Yamada, M. Kondo, R. Miyasato, Y. Naka, J.-I. Mamiya, M. Kinoshita, A. Shishido, Y. Yu, C. J. Barrett and T. Ikeda, *J. Mater. Chem.*, 2009, 19, 60.
[27] A. Priimagi, A. Shimamura, M. Kondo, T. Hiraoka, S. Kubo, J.-I. Mamiya, M. Kinoshita, T. Ikeda and A. Shishido, *ACS Macro Lett.*, 2012, 1, 96.
[28] M. Yamada, M. Kondo, J.-I. Mamiya, Y. Yu, M. Kinoshita, C. J. Barrett and T. Ikeda, *Angew. Chem. Int. Ed.*, 2008, 47, 4986.
[29] J. Küpfer and H. Finkelmann, *Makromol. Chem. Rapid Commun.*, 1991, 12, 717.
[30] P. G. de Gennes, *C. R. Acad. Sci.*, Paris, 1975, 281, 101.
[31] M. Warner and E. M. Terentjev, *Liquid Crystal Elastomers*, Claredon, 2003.
[32] H. Wermter and H. Finkelmann, *e*-polymers, 2001, 13, 1.
[33] D. L. Thomsen, P. Keller, J. Naciri, R. Pink, H. Jeon, D. K. Shenoy and B. R. Ratna, *Macromolecules*, 2001, 34, 5868.
[34] D. K. Shenoy, D. L. Thomsen, A. Srinivasan, P. Keller and B. R. Ratna, *Sensors and Actuators A: Phys.*, 2002, 96, 184.
[35] C. M. Spillmann, J. Naciri, M.-S. Chen, A. Srinivasan and B. R. Ratna, *Liq. Cryst.*, 2006, 33, 373.
[36] C. M. Spillmann, J. Naciri, B. D. Martin, W. Farahat, H. Herr and B. R. Ratna, *Sensors and Actuators A: Phys.*, 2007, 133, 500.
[37] P. M. Hogan, A. R. Tajbakhsh and E. M. Terentjev, *Phys. Rev. Lett. E*, 2002, 65, 041720.
[38] J. Cviklinski, A. R. Tajbakhsh and E. M. Terentjev, *Eur. Phys. J. E*, 2002, 9, 427.
[39] H. Finkelmann, E. Nishikawa, G. G. Pereira and M. Warner, *Phys. Rev. Lett.*, 2001, 87, 015501-1.
[40] P. J. Flory and J. Rehner, *J. Chem. Phys.*, 1943, 11, 521.
[41] P. J. Flory, *J. Chem. Phys.*, 1950, 18, 108.
[42] N. A. Neuburger and B. E. Eichinger, *Macromolecules*, 1988, 21, 3060.
[43] B. Erman and M. Baysal, *Macromolecules*, 1985, 18, 1696.
[44] A. Greve and H. Finkelmann, *Macromol. Chem. Phys.*, 2001, 202, 2926.
[45] C. D. Eisenbach, *Makromol. Chem.*, 1978, 179, 2489.
[46] M. G. Evans and M. Polanyi, *Trans. Faraday Soc.*, 1935, 31, 875.
[47] H. Eyring, *J. Chem. Phys.*, 1935, 3, 107.
[48] J. Garcia-Amorós, H. Finkelmann and D. Velasco, *J. Mater. Chem.*, 2011, 21, 1094.
[49] J. Garcia-Amorós, M. Martínez, H. Finkelmann and D. Velasco, *J. Phys. Chem. B*, 2010, 114, 1287.

[50] J. Garcia-Amorós, H. Finkelmann and D. Velasco, *Phys. Chem. Chem. Phys.*, 2011, 13, 11233.
[51] P. Beyer and R. Zentel, *Macromol. Rapid Commun.*, 2005, 26, 874.
[52] M. Camacho-López, H. Finkelmann, P. Palffy-Muhoray and M. Shelley, *Nat. Mater.*, 2004, 3, 307.
[53] C. L. M. Harvey and E. M. Terentjev, *Eur. Phys. J. E*, 2007, 23, 185.
[54] C. D. Eisenbach, *Polymer*, 1980, 21, 1175.
[55] C. J. Barrett, A. Natansohn and P. Rochon, *Chem. Mater.*, 1995, 7, 899.
[56] J. Garcia-Amorós, H. Finkelmann and D. Velasco, *Chem. Eur. J.*, 2011, 17, 6518.
[57] J. Garcia-Amorós, A. Sánchez-Ferrer, W. A. Massad, S. Nonell and D. Velasco, *Phys. Chem. Chem. Phys.*, 2010, 12, 13238.
[58] J. Garcia-Amorós, A. Piñol, H. Finkelmann and D. Velasco, *Org. Lett.*, 2011, 13, 2282.